AEM
Journals.ASM.org

A Novel DNA-Binding Protein, PhaR, Plays a Central Role in the Regulation of Polyhydroxyalkanoate Accumulation and Granule Formation in the Haloarchaeon *Haloferax mediterranei*

Shuangfeng Cai,[a,b] Lei Cai,[a,c] Dahe Zhao,[a,b] Guiming Liu,[a,b] Jing Han,[a] Jian Zhou,[a] Hua Xiang[a,b]

State Key Laboratory of Microbial Resources, Institute of Microbiology, Chinese Academy of Sciences, Beijing, People's Republic of China[a]; University of Chinese Academy of Sciences, Beijing, People's Republic of China[b]; School of Food Science and Biotechnology, Zhejiang Gongshang University, Hangzhou, People's Republic of China[c]

Polyhydroxyalkanoates (PHAs) are synthesized and assembled as PHA granules that undergo well-regulated formation in many microorganisms. However, this regulation remains unclear in haloarchaea. In this study, we identified a PHA granule-associated regulator (PhaR) that negatively regulates the expression of both its own gene and the granule structural gene *phaP* in the same operon (*phaRP*) in *Haloferax mediterranei*. Chromatin immunoprecipitation-quantitative PCR (ChIP-qPCR) assays demonstrated a significant interaction between PhaR and the *phaRP* promoter *in vivo*. Scanning mutagenesis of the *phaRP* promoter revealed a specific *cis*-element as the possible binding position of the PhaR. The haloarchaeal homologs of the PhaR contain a novel conserved domain that belongs to a swapped-hairpin barrel fold family found in AbrB-like proteins. Amino acid substitution indicated that this AbrB-like domain is critical for the repression activity of PhaR. In addition, the *phaRP* promoter had a weaker activity in the PHA-negative strains, implying a function of the PHA granules in titration of the PhaR. Moreover, the *H. mediterranei* strain lacking *phaR* was deficient in PHA accumulation and produced granules with irregular shapes. Interestingly, the PhaR itself can promote PHA synthesis and granule formation in a PhaP-independent manner. Collectively, our results demonstrated that the haloarchaeal PhaR is a novel bifunctional protein that plays the central role in the regulation of PHA accumulation and granule formation in *H. mediterranei*.

Polyhydroxyalkanoates (PHAs) are biodegradable polyesters synthesized by most genera of bacteria (1, 2) and some archaea (3–5). PHAs are accumulated as storage compounds of energy and carbon under imbalanced growth conditions (i.e., when nutrients such as nitrogen, phosphorus, or oxygen are limited but the carbon sources are in excess) (6).

PHAs are often deposited in the cytoplasm as water-insoluble inclusions that are called PHA granules (6). Native PHA granules are found to be composed of 97.5% PHA, 2% proteins, and likely some amount of lipids (7). At least four types of proteins were found to be the PHA granule-associated proteins (PGAPs) in bacteria: PHA synthases, PHA depolymerases, regulators, and structural proteins (phasins [PhaPs]) (8, 9). In recent years, increasing new roles have been found for the PGAPs. Besides the classical phasin role of preventing PHA granules from coalescing, two distinct phasin-like proteins, PhaM and PhaF, have also been characterized as being crucial for granule distribution during cell division (10, 11).

The PGAPs play important roles in PHA synthesis, PHA utilization, and granule formation and distribution (8, 9, 12), among which the regulatory proteins are responsible for ensuring the proper formation of PHA granules by influencing the expression of both phasins and themselves (13–17). A classic regulation model was presented in a poly(3-hydroxybutyrate) (PHB [a type of PHA])-accumulating bacterium, *Ralstonia eutropha* H16 (9). Briefly, the cytoplasmic regulator PhaR could bind to the promoter of *phaP* as well as the promoter of its own gene to repress their transcription. When cells start accumulating PHA, PhaR attaches to the PHA granules, which results in a lower cytoplasmic PhaR level. The block of the expression of *phaP* and *phaR* is released, and the cells start synthesizing more PhaP and PhaR to coat the growing PHA granules. PhaP is usually more abundant than PhaR and possesses a higher hydrophobic affinity to PHA granules. When the PHA granules reach a proper size, there is no more room on PHA granules for the excess PhaR to attach. The cytoplasmic PhaR concentration returns to a higher level to resume the repression of the transcription of both *phaP* and *phaR*. This tight regulation by PhaR ensures a well-organized granule formation process, in which sufficient PhaP proteins are produced to coat the newly synthesized PHAs, with few free PhaP present in the cytoplasm (9).

Unlike bacterial PGAPs, there has been little study of the archaeal PGAPs until recently. In our previous studies, five PGAPs were identified in a haloarchaeon, *Haloferax mediterranei*, which accumulates poly(3-hydroxybutyrate-*co*-3-hydroxyvalerate) (PHBV [a type of PHA]) and shows potential for industrial applications (18–20). Besides the PHA synthase subunits (PhaC and PhaE) and a putative enoyl coenzyme A (enoyl-CoA) hydratase (MaoC), two conserved hypothetical proteins (encoded by HFX_5218 and

Received 3 September 2014 **Accepted** 21 October 2014
Accepted manuscript posted online 24 October 2014
Citation Cai S, Cai L, Zhao D, Liu G, Han J, Zhou J, Xiang H. 2015. A novel DNA-binding protein, PhaR, plays a central role in the regulation of polyhydroxyalkanoate accumulation and granule formation in the haloarchaeon *Haloferax mediterranei*. Appl Environ Microbiol 81:373–385. doi:10.1128/AEM.02878-14.
Editor: M. Kivisaar
Address correspondence to Hua Xiang, xiangh@im.ac.cn.
Supplemental material for this article may be found at http://dx.doi.org/10.1128/AEM.02878-14.

doi:10.1128/AEM.02878-14

HFX_5219) were also separated from the PHA granules of *H. mediterranei*. The protein encoded by HFX_5219 was identified to be the major phasin (PhaP) that could prevent the aggregation of PHA granules (20). HFX_5218 encodes a small protein that was temporarily named GAP12 (12.0 kDa). The *gap12* gene was revealed to be cotranscribed with *phaP*, but its function is still unknown (20). Characterization of the GAP12 separated from PHA granules might provide important hints for the exploration of the regulation of PHA biosynthesis and granule formation in haloarchaea.

In this study, using a combined approach of gene expression, gene knockout, promoter activity analysis, and a chromatin immunoprecipitation-quantitative PCR (ChIP-qPCR) assay, the GAP12 protein was identified as a regulator and renamed PhaR, which directly binds to the promoter of *phaRP* and negatively regulates this operon. In addition, the *cis*-elements of the *phaRP* promoter were identified by site-directed mutagenesis, and the effects of PhaR on the PHA accumulation and granule formation were further demonstrated by gas chromatography and electron microscopy analyses. Therefore, the identification and characterization of the haloarchaeal type of phasin regulator PhaR, which is phylogenetically distinct from the bacterial counterpart, have provided new insights into the regulation of PHA synthesis in haloarchaea.

MATERIALS AND METHODS

Strains and culture conditions. The strains used in this study are listed in Table 1. *Escherichia coli* JM109 was used for cloning procedures and was grown in lysogeny broth (LB) medium at 37°C (21). *H. mediterranei* DF50, a uracil-auxotrophic (Δ*pyrF*) strain of *H. mediterranei* ATCC 33500 (22), and its derivative mutants were cultivated at 37°C in nutrient-rich AS-168L medium (20). *H. mediterranei* strains carrying expression plasmids were cultivated in AS-168SYL medium (with yeast extract omitted from AS-168L) (20). For PHA accumulation analysis, the culture procedures were similar to those described previously (20). Briefly, *H. mediterranei* was first grown in AS-168L for 2 days and then was inoculated into a modified PHA production medium, named MGF medium, containing (per liter) 110 g NaCl, 9.6 g $MgCl_2$, 14.4 g $MgSO_4$, 5 g KCl, 1 g $CaCl_2$, 3 g yeast extract, 2 g NH_4Cl, 0.0375 g KH_2PO_4, 10 g glucose, 15 g PIPES [piperazine-*N*,*N*′-bis(2-ethanesulfonic acid)], 0.008 g NH_4^+-Fe(III) citrate, and 1 ml trace element solution SL-6 (pH 7.2) (18). For AS-168SYL seed cultures, yeast extract was also omitted from the MGF medium. When needed, ampicillin, uracil, and 5-fluoroorotic acid (5-FOA) were added to the medium at final concentrations of 100, 50, and 250 mg/liter, respectively.

Construction of mutants. The plasmids and primers used in this study are listed in Tables 1 and 2, respectively. The in-frame gene deletion and gene expression in *H. mediterranei* were carried out as previously described (20, 22, 23).

For construction of the green fluorescent protein (GFP) reporter plasmid pRF, a 168-bp DNA fragment upstream of the *phaR* open reading frame (ORF) (the promoter of the *phaRP* operon, named P_{phaRP}) was linked with the coding region of a soluble modified red-shifted green fluorescent protein (smRSGFP [simply named "GFP" here]) (24), and was cloned into the expression plasmid pWL502 (20). For another reporter plasmid, pEF, the P_{phaRP} fragment in pRF was replaced by a 189-bp DNA fragment upstream of the *phaE* ORF. To introduce mutations into DNA fragments, the site-directed mutagenesis was performed using a DpnI-mediated method as described previously (25). Briefly, the 168-bp P_{phaRP} fragment was cloned into the pGEM-T Easy vector (Promega), and the resultant plasmid, pT-Rpro, was used as the PCR template for the site-directed mutagenesis of P_{phaRP}. The P_{phaRP} fragments with desired mutations together with the *gfp* fragment were subcloned into pWL502 to generate the plasmids pD41, pD86, and pM1 to pM16, respectively.

For the amino acid residue substitutions in PhaR, a knock-in plasmid, pR-IN, which possesses a 1.2-kb DNA fragment containing the *phaR* ORF and its upstream and downstream regions, was used as the template. The substitutions were introduced independently into each plasmid by DpnI-mediated site-directed mutagenesis. The resultant plasmids (e.g., pR-IN-E24A) were, respectively, transferred into the *H. mediterranei* strain with *phaR* deleted and integrated into the chromosome to generate the corresponding strains, which express the desired PhaR mutants (e.g., $PhaR^{E24A}$).

For the overexpression of *phaR* or *phaP*, each ORF region was inserted into the pSCM307 plasmid (26). Then, the corresponding fragments containing both the *hsp5* promoter region and the ORF region of *phaP* (or *phaR*) were subcloned into the plasmid pWL502 (or pRF), resulting in plasmid pHP (or pHRRF). For the complementary expression of *phaR* or *phaRP*, a fragment containing the region of the native promoter and the ORF of *phaR* (or the ORFs of *phaRP*) was cloned into pWL502 to generate plasmid pWLR (or pWLRP).

All PCR-amplified sequences were verified by DNA sequencing. The plasmid transformation of *H. mediterranei* was performed by a polyethylene glycol-mediated transformation method (27).

Promoter activity assays. *H. mediterranei* strains harboring the GFP reporter plasmids were cultured at 37°C in AS-168SYL medium. Cells (100 μl/well) from certain growth phases were transferred into 96-well plate to measure the turbidity (optical density at 600 nm [OD_{600}]) and the fluorescence intensity (excitation, 488 nm; emission, 509 nm) using a Synergy H4 hybrid microplate reader (BioTek Instruments, Inc., Winooski, VT) (24, 28), with AS-168SYL medium serving as the blank control. The fluorescence intensity was normalized against the cell density (per OD_{600} of 0.1) and expressed as relative fluorescence units (RFU). At least three independent biological replicates were performed.

RNA extraction, CR-RT-PCR, and Northern blot analysis. The total RNA of *H. mediterranei* cells in late-exponential phase was extracted with TRIzol reagent (Invitrogen) (29).

For the identification of the transcription start site (TSS), the circularized RNA reverse transcription-PCR (CR-RT-PCR) method was carried out as previously described (30). After the reverse transcription of self-ligated RNA with random hexamer primers, the cDNA was used as the PCR template. The PCR products amplified with the primer pair phaRP-CRRT-F/phaRP-CRRT-R were cloned into the pGEM-T Easy vector to determine the TSS by DNA sequencing.

For Northern blot analysis, 4 μg of each RNA sample was separated on a 4% denaturing polyacrylamide gel (7 M urea, 0.5× Tris-borate-EDTA [TBE] buffer) and transferred onto the nylon membranes using a semidry transfer cell (Bio-Rad). The probes used to detect the expression of *phaP* and the internal control 7S RNA were amplified by the primer pairs phaP-NB-F/phaP-NB-R and 7S-NB-F/7S-NB-R, respectively. The probes were labeled with biotin-11-dUTP (R0081; Thermo Scientific) by PCR. After the cross-linking of RNA onto the membranes by UV, the membranes were hybridized with the labeled probes. The prehybridization, hybridization, and washing procedures were performed as previously described (29). The biotin was detected using the Pierce chemiluminescent nucleic acid detection module (Thermo Scientific, Rockford, IL).

Protein expression and purification, antiserum preparation, and Western blot analysis. The coding regions of *phaR* and *phaP* amplified by the primer pairs PhaR-28a-F/PhaR-28a-R and PhaP-28a-F/PhaP-28a-R, respectively, were inserted into the vector pET-28a (Novagen). The resultant expression plasmids, pET-28aR and pET-28aP, were transferred into *E. coli* BL21(DE3), respectively. Expression and purification of the PhaR-His_6 and PhaP-His_6 proteins, as well as the preparation of the corresponding antisera were performed as previously described (31).

For Western blot analysis, the cells cultivated in MGF medium were collected in the stationary phase (after cultivation for approximately 3 days). The cell pellets were dissolved in 8 M urea buffer and homogenized

TABLE 1 Strains and plasmids used in this study

Strain or plasmid	Relevant characteristics	Source or reference
Strains		
E. coli		
JM109	*recA1 supE44 endA1 hsdR7 gyrA96 relA1 thi*	21
BL21(DE3)	F^- *ompT* $hsdS_B(r_B^- m_B^-)$ *dcm gal* (DE3)	Novagen
H. mediterranei		
DF50	*pyrF* deletion mutant of *H. mediterranei* ATCC 33500	22
Δ*phaP* mutant	*phaP* deletion mutant of *H. mediterranei* DF50	20
Δ*phaR* mutant	*phaR* deletion mutant of *H. mediterranei* DF50	This study
Δ*phaRP* mutant	*phaRP* deletion mutant of *H. mediterranei* DF50	This study
Δ*phaEC* mutant	*phaEC* deletion mutant of *H. mediterranei* DF50	This study
Δ*phaPEC* mutant	*phaPEC* deletion mutant of *H. mediterranei* DF50	This study
Δ*phaRPEC* mutant	*phaRPEC* deletion mutant of *H. mediterranei* DF50	This study
E24A	DF50 strain with PhaR carrying E24A mutation	This study
Q28A	DF50 strain with PhaR carrying Q28A mutation	This study
Q30A	DF50 strain with PhaR carrying Q30A mutation	This study
R32A	DF50 strain with PhaR carrying R32A mutation	This study
K67A	DF50 strain with PhaR carrying K67A mutation	This study
R75A	DF50 strain with PhaR carrying R75A mutation	This study
E82A	DF50 strain with PhaR carrying E82A mutation	This study
R83A	DF50 strain with PhaR carrying R83A mutation	This study
Plasmids		
pHFX	4.0-kb integration vector containing *pyrF* and its native promoter, Amp^r	22
pWL502	7.8-kb expression vector containing *pyrF* and its native promoter, Amp^r	20
pSCM307	8.2-kb shuttle vector containing promoter of *hsp5* of *Halobacterium* sp. strain NRC-1, Amp^r	26
pJAM1020	10.7-kb expression plasmid containing smRSGFP gene, Amp^r	24
pM1915	8.8-kb expression vector pWL502 containing smRSGFP gene and mutated promoter of PTS	28
pGEM-T Easy	3.0-kb cloning vector, Amp^r	Promega
pET-28a	5.4-kb IPTG-inducible expression vector with His_6 tag	Novagen
pDR	5.6-kb integration vector of pHFX for knockout of *phaR*	This study
pDRP	5.6-kb integration vector of pHFX for knockout of *phaRP*	This study
pDEC	5.3-kb integration vector of pHFX for knockout of *phaEC*	This study
pDPEC	5.4-kb integration vector of pHFX for knockout of *phaPEC*	This study
pDRPEC	5.4-kb integration vector of pHFX for knockout of *phaRPEC*	This study
pR-IN	5.2-kb integration vector of pHFX for knock-in of *phaR*	This study
pRF	8.7-kb expression vector pWL502 containing smRSGFP gene and the *phaRP* promoter (−151 to +17)	This study
pEF	8.7-kb expression vector pWL502 containing smRSGFP gene and *phaEC* promoter	This study
pWLR	8.4-kb expression vector pWL502 containing *phaR* and *phaRP* promoter	This study
pWLP	8.5-kb expression vector pWL502 containing *phaP* and *phaRP* promoter	20
pWLRP	8.8-kb expression vector pWL502 containing *phaRP* and *phaRP* promoter	This study
pHP	8.4-kb expression vector pWL502 containing *phaP* and *hsp5* promoter	This study
pHRRF	9.2-kb pRF-derived vector for additional expression of *phaR* under *hsp5* promoter	This study
pRmyc	8.3-kb pWL502 derived vector, expressing *phaR-myc* under mutated PTS promoter from pM1915	This study
pT-Rpro	2.9-kb pGEM-T Easy-derived cloning vector of *phaRP* promoter	This study
pM1 to pM16	8.7-kb pRF-derived vectors with mutations introduced into *phaRP* promoter	This study
pD41	8.6-kb pRF-derived vector with *phaRP* promoter truncated (−41 to +17)	This study
pD86	8.6-kb pRF-derived vector with *phaRP* promoter truncated (−86 to +17)	This study
pET-28aR	5.7-kb pET-28a-derived vector, expressing *phaR*-His_6	This study
pET-28aP	5.8-kb pET-28a derived vector, expressing *phaP*-His_6	This study
pR-IN-E24A	5.2-kb integration vector of pHFX for knock-in of *phaR* with E24A mutation	This study
pR-IN-Q28A	5.2-kb integration vector of pHFX for knock-in of *phaR* with Q28A mutation	This study
pR-IN-Q30A	5.2-kb integration vector of pHFX for knock-in of *phaR* with Q30A mutation	This study
pR-IN-R32A	5.2-kb integration vector of pHFX for knock-in of *phaR* with R32A mutation	This study
pR-IN-K67A	5.2-kb integration vector of pHFX for knock-in of *phaR* with K67A mutation	This study
pR-IN-R75A	5.2-kb integration vector of pHFX for knock-in of *phaR* with R75A mutation	This study
pR-IN-E82A	5.2-kb integration vector of pHFX for knock-in of *phaR* with E82A mutation	This study
pR-IN-R83A	5.2-kb integration vector of pHFX for knock-in of *phaR* with R83A mutation	This study

TABLE 2 Oligonucleotides used in this study

Primer	5′→3′ sequence[a]
Gene knockout and knock-in	
phaR-DF1	ATAGGTACCCGGTGTCACCTGGATT
phaR-DR1	ATAGGATCCGTCGTTCGTCATCTCCT
phaR-DF2	TATGGATCCAGTGAACAAGCCAACCC
phaR-DR2	ATACTGCAGGGTCTCCTCTATCTCCTGT
phaRP-DF1	GATGGTACCACCATCGGCGTTCGTAA
phaRP-DR1	GCAGGATCCCTCCTAACTCGGTGTTGT
phaRP-DF2	TCTGGATCCCTACAGGAGATAGAGGAG
phaRP-DR2	CGACAAGCTTCTTCGTTTGGGGTTTTGC
phaEC-DF1	GATGGTACCCGATGGGTGACTTCC
phaEC-DR1	TCTGGATCCCCGACAGACTACTCCG
phaEC-DF2	TTAGGATCCCGTGGGTTGAACAGG
phaEC-DR2	GCCGAAGCTTGATAGCACAGCGAAA
phaPEC-DF1	ATAGGTACCCCTCGTCTCCGTCCAGTC
phaPEC-DR1	GAGGGATCCTCACTCATTTGAATCACC
R-IN-F	ATAGGTACCCGAGTCGTCGTAGGCA
R-IN-R	ATAGGATCCACTACTCCGGCGTGTC
Gene complementary expression	
phaR-ex-F	GCAGGTACCCTTATGTACTTCGGTATGTG
phaR-ORF-R	GTCGGATCCTCACTCATTTGAATCACCAC
phaP-ORF-R	TATGGATCCTCTCGGGCGGGCTAAA
Gene overexpression	
phaR-ORF-F	GTACTCGCATATGACGAACGACTCAAACGATGC
phaR-ORF-R	GTCGGATCCTCACTCATTTGAATCACCAC
phaP-ORF-F	GTACTCGCATATGAGTGAACAAGCCAACCC
phaP-ORF-R	TATGGATCCTCTCGGGCGGGCTAAA
Promoter GFP fusion reporter	
phaR-Pro-F	CAGGGTACCCCCAACTTATGTACTTCG
phaR-Pro-R	CGCAAGCTTGTCGTTCGTCATCTCCT
gfp-ORF-F	CCCAAGCTTAGTAAAGGAGAAGAACTTTTCAC
gfp-ORF-R	CGGGATCCTTATTTGTATAGTTCATCCATGC
phaE-Pro-F	CTAGGTACCGAGGAGAACGCAGACG
phaE-Pro-R	CGCAAGCTTTTGTGACATGGGCATA
PhaR-His_6 and PhaP-His_6 expression	
phaR-28a-F	GTACTCGCATATGACGAACGACTCAAACG
phaR-28a-R	GGACTCGAGTCACTCATTTGAATCACCA
phaP-28a-F	GTACTCGCATATGAGTGAACAAGCCAACC
phaP-28a-R	AGACTCGAGCTACTCCGGCGTGTCTGGT
PhaR-Myc fusion expression	
M1915-Pro-F	CGGGGTACCCGAGGTAACCACTGTACG
M1915-Pro-R	CATGCCATGGCATAGTGTTGCCAACCCTCTGC
phaR-ORF-F2	CATGCCATGGACGAACGACTCAAACGAT
phaR-ORF-R2	CGCAAGCTTCTCATTTGAATCACCACG
myc1-ct-F	AGCTTGAGCAGAAGCTCATCAGCGAGGAGGATCTGTGAG
myc1-ct-R	GATCCTCACAGATCCTCCTCGCTGATGAGCTTCTGCTCA
Northern blot probe	
phaP-NB-F	ACAAGCCAACCCATTCA
phaP-NB-R	CCAGGTCTGTTCGGTCAT
7S-NB-F	TAGGTCGGGCAGTTA
7S-NB-R	GCGACGCACGTCCGATGGT
CR-RT-PCR and qRT-PCR	
phaRP-CRRT-F	CCTGGGATGTCATGGAAG
phaRP-CRRT-R	GCTGTCTGAAACACCCGTAC
16S-qF	CGTCCGCAAGGATGAAA
16S-qR	CAGCGTCGTGGTAAGGT

(Continued on following page)

TABLE 2 (Continued)

Primer	5′→3′ sequence[a]
phaR-Pro-qF	CCCAACTTATGTACTTCGG
phaR-Pro-qR	GTCGTTCGTCATCTCCTA
glpR-Pro-qF	CCGTTTCTCGTTCAGTTTC
glpR-Pro-qR	CCTCGTTAGGTGGATGGTA
Truncation of *phaRP* promoter	
phaR-Pro-41F	CAGGGTACCCGAAGGGAACATATATG
phaR-Pro-86F	CAGGGTACCCGGCTTCTACACCATAC
phaR-Pro-R	CGCAAGCTTGTCGTTCGTCATCTCCT
Site-directed mutation of *phaRP* promoter[b]	
M1-F	CGAAGGGAACATATATGTTACTG**ACC**GTACAACACCGAGTTAGGAG
M2-F	CGAAGGGAACATATAT**TGG**ACTGCAGGTACAACAC
M3-F	TGTCGAAGGGAACATA**GCGTGG**ACTGCAGGTACAACAC
M4-F	CCACTAAATGGTGTCG**CA**TG**TC**ACATATATGTTACTGCAG
M5-F	CCATCTGATACCACTAA**CGCTGTG**CGAAGGGAACATATA
M6-F	GATACCATCTGATACCA**AGCC**ATGGTGTCGAAGGGA
M7-F	CCATACGATACCATCTG**CTCAAC**CTAAATGGTGTCGAAG
M8-F	ACACCATACGATACCA**GAGT**ATACCACTAAATGGTGT
M9-F	GCTTCTACACCATACG**CGCAAC**TCTGATACCACTAAATG
M10-F	CGGCTTCTACACCAT**CAT**ATACCATCTGATACCAC
M11-F	GATTTTTGCCGGCTTCT**CACAACG**ACGATACCATCTGATAC
M13-F	GGGGATTTTTGCCGGC**GGAG**ACACCATACGATACC
M14-F	CAGGCAGGGGATTTTTG**AC**T**GA**TTCTACACCATACGATACC
M15-F	TGCCAGGCAGGGG**CT**G**T**G**T**GCCGGCTTCTACAC
M16-F	ACTGAGTGCCAGGC**C**G**T**G**T**ATTTTTGCCGGCTTCT
PhaR point mutation[b]	
E24A-F	GATGCAGAAAGCCAGC**GCT**GAGTTCACCCAACAAC
Q28A-F	CAGCGAAGAGTTCACC**GCT**CAACAACTCCGTCTGT
Q30A-F	AGAGTTCACCCAACAA**GC**ACTCCGTCTGTTCGA
R32A-F	CACCCAACAACAACTC**GC**TCTGTTCGAACAACTG
K67A-F	CAAACCGCGGTCTTC**GC**AACGCGCGTGCAGA
R75A-F	TGCAGAGTGGGGGG**GCT**ATCAGCATCCCCGAC
E82A-F	CATCCCCGACGCTG**C**GCGCGATGCCCTC
R83A-F	ATCCCCGACGCTGAG**GCT**GATGCCCTCGACATC

[a] Sequences representing restriction sites are underlined.
[b] The substituted nucleotides in the sense primers (M1-F to M16-F and E24A-F to R83A-F) are indicated by boldface letters. The corresponding antisense primers are not listed because they are exactly the reverse complements of the sense primers.

by ultrasonication. Cell debris was removed by centrifugation. The protein concentrations in the extracts were measured with a bicinchoninic acid protein assay kit (Applygen Technologies, Inc., Beijing, China). For each set of experiments, the same amount of total proteins (30 μg for detection of PhaP and 100 μg for detection of PhaR and Myc-tag) was resolved by 14% SDS-PAGE and analyzed by Western blotting with antibodies against PhaR, PhaP, or Myc tag (M20002; Abmart), performed as previously described (31).

ChIP and qPCR assays. For chromatin immunoprecipitation (ChIP) analysis, a C-terminal tagged PhaR-Myc protein was expressed in a *phaR* knockout mutant. The cells from the late-exponential-phase culture of *H. mediterranei* were used for ChIP analysis according to Wilbanks et al. (32). Briefly, cells were fixed in 1% (vol/vol) formaldehyde for 10 min and then treated with 125 mM glycine for 5 min and washed twice with TBSL buffer (20). Approximately 10^{10} cells were resuspended in 700 μl cold lysis buffer (32) containing 1× protease inhibitor cocktail (PIC [Sigma]). The lysate was then sonicated (4 s on/5 s off, 4-min cycles, 20% power setting) using a JY92-IIDN ultrasonic homogenizer (Ningbo Scientz Biotechnology Co., Ltd., Ningbo, China) to shear the DNAs to lengths between 200 and 1,000 bp. After centrifugation (at 16,000 × *g* at 4°C) for 3 min, 50 μl of the supernatant was saved as the input sample. The rest of the supernatant was mixed with 2 μl of anti-Myc antibody and 30 to ~40 μl of protein A Sepharose CL-4B beads (GE Healthcare), which were preblocked with 5 mg/ml bovine serum albumin (BSA) in phosphate-buffered saline. The mixture was incubated overnight at 4°C. The following bead-washing steps and the elution step (with 50 μl of elution buffer) were performed exactly like the protocol reported by Wilbanks et al. (32). Tris-EDTA (TE)-SDS (32) (180 μl) was added to the eluates (20 μl) and the input sample (20 μl), respectively, to reverse the cross-linking by incubation overnight at 65°C. The DNA was purified with an E.Z.N.A. Cycle-Pure kit (Omega Bio-Tek).

The ChIP DNA fractions were analyzed by using quantitative real-time PCR (qPCR) to measure the enrichment of genomic DNA regions of interest with the primers shown in Table 2. The qPCR was performed on Rotor-Gene Q real-time cycler (Qiagen, Valencia, CA) with Kapa SYBR Fast qPCR master mix (2×) (KM4101; Kapa Biosystems) using a three-step PCR procedure (including initial denaturation at 95°C for 5 min followed by 40 cycles of denaturation at 95°C for 15 s, annealing at 54°C for 20 s, and synthesis at 72°C for 30 s). Product specificity was confirmed by melting curve analysis. A 16S rRNA gene region (positions+836 to +980 relative to the TSS) was used to normalize the qPCR results of each ChIP sample. The enrichment of DNA fragments was analyzed with the input DNA samples serving as controls. Samples were analyzed in tripli-

cate from three independent ChIP assays, and representative results from one biological replicate are presented.

PHA accumulation assay and TEM studies. After a 3-day's cultivation in MGF medium, the cells in the stationary phase were harvested for the PHA accumulation assay or for transmission electron microscopy (TEM) analysis. The PHA content and PHA composition analyses using gas chromatography were performed as previously described (31). The PHA granule morphology was observed through TEM analysis with a workflow in accordance with the procedure described previously (20, 33). Photomicrographs were taken with a Philips JEOL-1400 electron microscope.

Bioinformatics analysis. The codon adaptation index (CAI) was analyzed on the CAIcal server (http://genomes.urv.es/CAIcal/).

RESULTS

Identification of the AbrB-like protein PhaR and the promoter of the *phaRP* operon in *H. mediterranei*. We have previously reported a small protein GAP12 (110 amino acids [aa]), which was present in abundance on the PHA granule of *H. mediterranei*, with its coding gene cotranscribed with the phasin gene *phaP* (20). The *gap12-phaP* operon is located upstream of the *phaEC* operon that encodes the two subunits of PHA synthase (Fig. 1A). Conserved domain search analysis at NCBI revealed that the C-terminal portion of GAP12 has a putative DNA-binding domain consisting of swapped-hairpin barrel fold, which shows low homology (with an E value of 1.82e−05) to the corresponding domain of the AbrB (antibiotic resistance protein B) superfamily of regulators (34), implying a regulatory-related function of GAP12. Thus, the GAP12 was renamed PhaR, and the *gap12-phaP* operon was renamed the *phaRP* operon (Fig. 1A).

To explore the function of PhaR and its expression profiles, a GFP-based reporter system was constructed to conveniently monitor the activity of the *phaRP* promoter (P_{phaRP}). First, the TSS of the *phaRP* cotranscript was analyzed using a CR-RT-PCR approach. An adenine residue at 5 bp upstream of the initiator ATG codon was determined as the TSS of *phaRP*, which revealed an extended 5′-untranslated region (5′-UTR) with the sequence AGGAG (Fig. 1B). A 168-bp region (positions −151 to +17 relative to the TSS of *phaRP*) joined with the *gfp* gene was used to construct the P_{phaRP}-*gfp*-fused reporter plasmid pRF (Fig. 1B and Fig. 2A). After plasmid pRF had been transferred into *H. mediterranei* DF50 (22), GFP could be visualized by fluorescence microscopy (see Fig. S1 in the supplemental material). The activity of the P_{phaRP} promoter was evaluated by quantifying the fluorescence signal with a fluorescence microplate reader.

The promoter activities of the P_{phaRP} were monitored during cell growth. As PHA is actively accumulated in the cells in the stationary phase and the promoter activity of P_{phaRP} is more stable at this phase, we primarily show or discuss the data obtained in the stationary phase. Remarkable fluorescence intensity (reaching values of over 10,000 RFU) was detected in the DF50/pRF strain, while the promoter of the *phaEC* operon only showed a weaker signal (up to approximately 500 RFU in the DF50/pEF strain) (Fig. 1C). These results reveal that P_{phaRP} exhibits a strong activity that is consistent with the high abundance of the PhaP protein.

Modulation of *phaRP* expression and its promoter activity by PhaR and PHA accumulation. Since PhaR is associated with the PHA granules, first the effect of PHA production on the *phaRP* expression level was analyzed. The PHA-accumulating haloarchaea possess a conserved *pha* gene cluster (*phaR-phaP-phaE-phaC*), including two operons, *phaRP* and *phaEC*, in *H. mediterranei* (Fig. 1A) (20). The deletion of the PHA synthase operon (*phaEC*) makes cells incapable of synthesizing PHA (35). The pRF plasmid was transferred to three PHA-negative mutants, including the Δ*phaEC*, Δ*phaPEC*, and Δ*phaRPEC* strains, and the expression levels of GFP were evaluated. The Δ*phaEC* and Δ*phaPEC* mutants both showed an approximately 2-fold decrease in the activity of the P_{phaRP} promoter compared with that of the same promoter in DF50 (Fig. 1D), implying that the expression of *phaRP* could be activated by the presence of PHA. In contrast, the further deletion of the *phaR* gene in Δ*phaPEC*, which resulted in the third PHA-negative mutant Δ*phaRPEC* strain, caused an increase of more than 4-fold in the activity of P_{phaRP} (Fig. 1D). These results suggest that when cells do not synthesize PHA, the expression of *phaRP* is suppressed, whereas the knockout of the *phaR* gene could relieve this suppression effect. Thus, the PhaR could be a negative regulator of the *phaRP* operon.

To further explore the function of PhaR, we also carried out an overexpression of *phaR* using a plasmid-based method. The overexpression plasmid pHRRF was derived from pRF, with *phaR* driven by a strong *hsp5* promoter at the EcoRI site of pRF

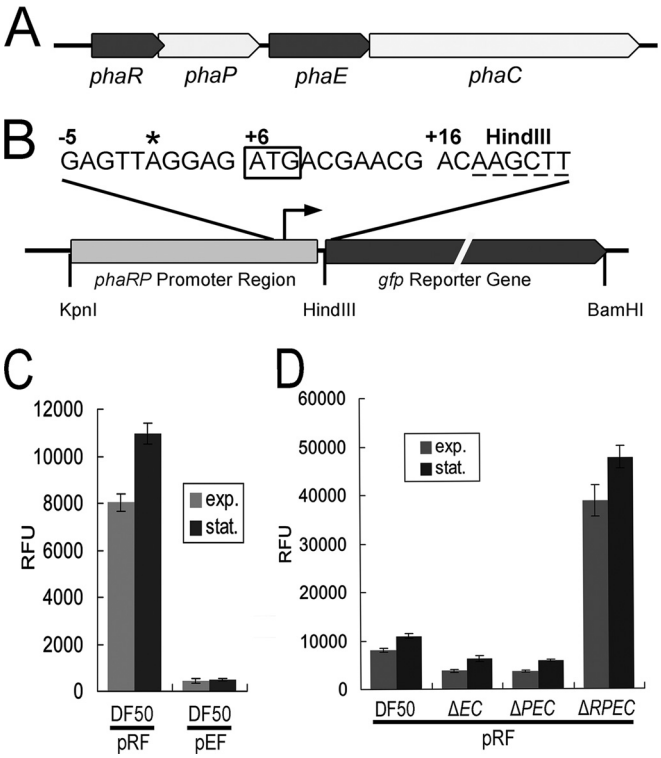

FIG 1 Expression-level analyses of *phaRP* using the *gfp* reporter system in strains with *pha* genes mutated. (A) Genetic organization of the *pha* gene cluster (*phaRP* and *phaEC*) in *H. mediterranei*. The arrows indicate the direction of gene transcription. (B) Schematic representation (not to scale) of the P_{phaRP}-*gfp* fusion in the reporter plasmid pRF. The transcription start site of the *phaRP* operon identified by CR-RT-PCR is indicated with an asterisk. The translation start codon of *phaR* (boxed) and the HindIII restriction site (dashed) are also shown. (C) Comparison of the promoter activities of the *phaRP* operon (pRF) and *phaEC* operon (pEF) in *H. mediterranei* strain DF50. (D) Comparison of the GFP expression levels of the *H. mediterranei* DF50, Δ*phaEC* (Δ*EC*), Δ*phaPEC* (Δ*PEC*), and Δ*phaRPEC* (Δ*RPEC*) strains harboring plasmid pRF. The promoter activities in both the exponential (exp.) phase and the stationary (stat.) phase are shown. Error bars show standard deviations ($n = 3$). RFU, relative fluorescence units.

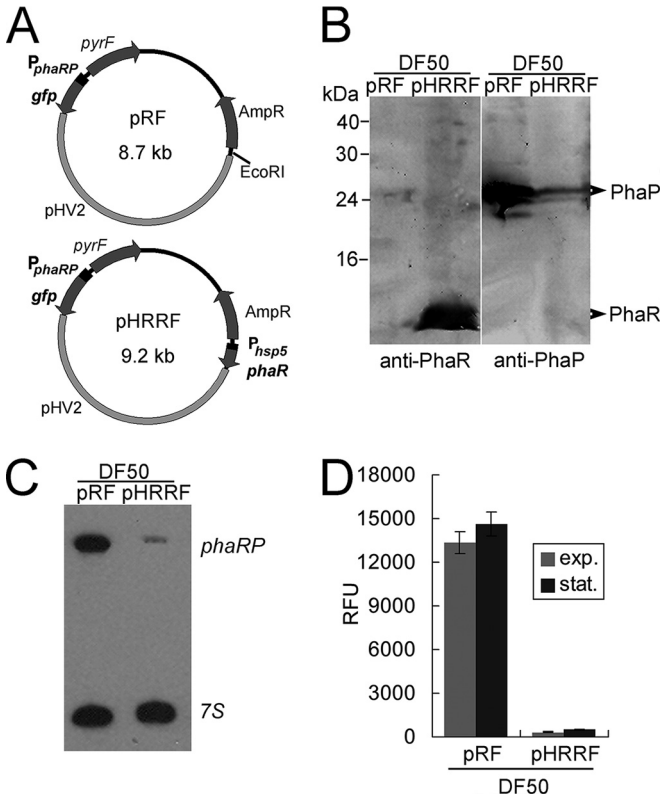

FIG 2 Expression-level analyses of *phaRP* in a *phaR* overexpression strain. (A) Schematic representation of the reporter plasmids pRF and pHRRF. The ampicillin resistance gene (AmpR), the *pyrF* gene, and the pHV2 replicon are labeled. The key genetic elements for the reporter system, including the *phaRP* promoter and the *gfp* ORF, are shown in both pRF and pHRRF. The *hsp5* promoter and the *phaR* ORF, which are elements further introduced at the EcoRI restriction site of pRF, are indicated in pHRRF. (B) Western blot analyses of PhaR and PhaP expression levels in the DF50/pRF and DF50/pHRRF strains. Cells were collected at the stationary phase. To detect PhaP and PhaR, crude extracts of 30 μg and 100 μg, respectively, were loaded for SDS-PAGE. (C) Northern blot analysis of the *phaRP* transcript in the DF50/pRF and DF50/pHRRF strains. The 7S transcript served as an internal control. (D) Comparison of the GFP expression levels of the DF50/pRF and DF50/pHRRF strains. The *phaRP* promoter activities in both the exponential (exp.) phase and the stationary (stat.) phase are shown. Error bars show standard deviations ($n = 3$).

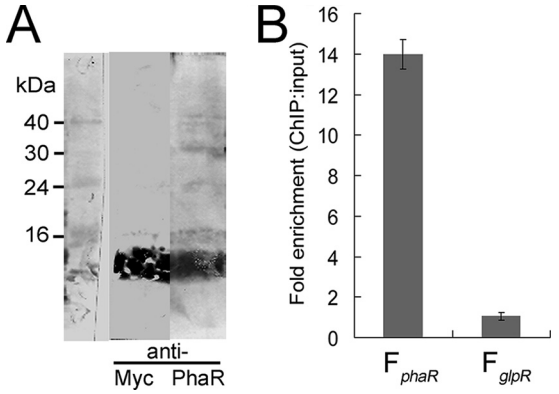

FIG 3 ChIP-qPCR assay for analysis of binding of PhaR with the promoter region of the *phaRP* operon. (A) Detection of PhaR-Myc fusion protein by Western blotting assay with anti-Myc and anti-PhaR antibodies, respectively. (B) DNA enrichment assay of the PhaR-Myc fusion protein. The fold enrichment of the *phaR* promoter region (F_{phaR}; 168 bp) and the *glpR* promoter region (F_{glpR}; 137 bp) is shown. The relative abundance of each region in both the ChIP and the input DNA samples was calculated by normalization to the abundance of the inner control region. Error bars show standard deviations ($n = 3$).

(Fig. 2A). The plasmid pHRRF was transferred into the DF50 strain to generate the DF50/pHRRF strain, and the influence of PhaR on the expression of *phaP* was investigated. The enhanced expression of *phaR* in DF50/pHRRF strain was revealed by Western blotting using anti-PhaR antibody, whereas the expression level of the major phasin PhaP was analyzed with anti-PhaP antibody (Fig. 2B). As shown in the Western blot results, overproduced PhaR in the cells strongly reduced the amount of PhaP (Fig. 2B). Further Northern blot analysis with a *phaP*-specific probe showed that in contrast to the high abundance of *phaRP* transcript in the DF50/pRF strain, only a negligible amount of *phaRP* mRNA was detected in the *phaR* overexpression strain DF50/pHRRF (Fig. 2C). These data indicate that PhaR controls the amount of the PhaP protein by inhibiting the expression of *phaRP* at the transcriptional level. Concomitant with these observations, in the DF50/pHRRF strain, the fluorescence signal driven by the P_{phaRP} promoter was strongly decreased to be a faint signal (200 to 300 RFU) by the larger amount of the PhaR protein (Fig. 2D), confirming the repression role of PhaR.

In conclusion, these results reveal that absence of PhaR could enhance the expression of *phaRP*, while excess of PhaR could reduce the expression, demonstrating that PhaR is a transcriptional repressor of both itself and *phaP*. In addition, the presence of PHA also could active the expression of *phaRP*, indicating that a PhaR titration effect of PHA granules plays an important role in the fine modulation of *phaRP* expression.

Direct binding of the regulator PhaR to the promoter of the *phaRP* operon *in vivo*. The above results demonstrated that overexpression of PhaR severely inhibited the transcription of *phaRP* operon. To determine whether the repression effect by PhaR occurs by interacting directly with the promoter region of the *phaRP* operon, we further performed a ChIP-qPCR assay.

First, we expressed a PhaR protein that was Myc tagged at its C terminus in a *phaR* knockout strain. The expression of the PhaR-Myc was driven by a strong constitutive promoter that is a mutated promoter of the phosphotransferase system (PTS) gene cluster from plasmid pM1915 (28). The successful expression of Myc-tagged PhaR was confirmed via Western blot analysis with anti-PhaR and anti-Myc antibodies, respectively (Fig. 3A). After using monoclonal anti-Myc antibodies to immunoprecipitate the Myc-tagged PhaR protein, the coprecipitated DNA was analyzed. Both the ChIP-extracted DNA and the input DNA were examined by qPCR. A 145-bp region, F_{16S}, from the 16S rRNA gene was used as an inner control to normalize all qPCR results. For the P_{phaRP} promoter, the qPCR product, F_{phaR}, was designed to span a region from −151 to +17 relative to the TSS of *phaRP*. A promoter region (F_{glpR}; −148 to −12 relative to the translation start site of *glpR*) of the *glpR* gene, which is functionally irrelevant to the PHA biosynthesis as shown in the microarray data of the Δ*phaEC* mutant (36), was chosen to be a distal/negative-control region. As shown in Fig. 3B, the fragment F_{phaR} was remarkably enriched (14.0-fold) by PhaR-Myc, while no significant enrichment (1.1-fold) of the distal/negative-control fragment F_{glpR} to PhaR-Myc was observed, demonstrating that PhaR interacts specifically with

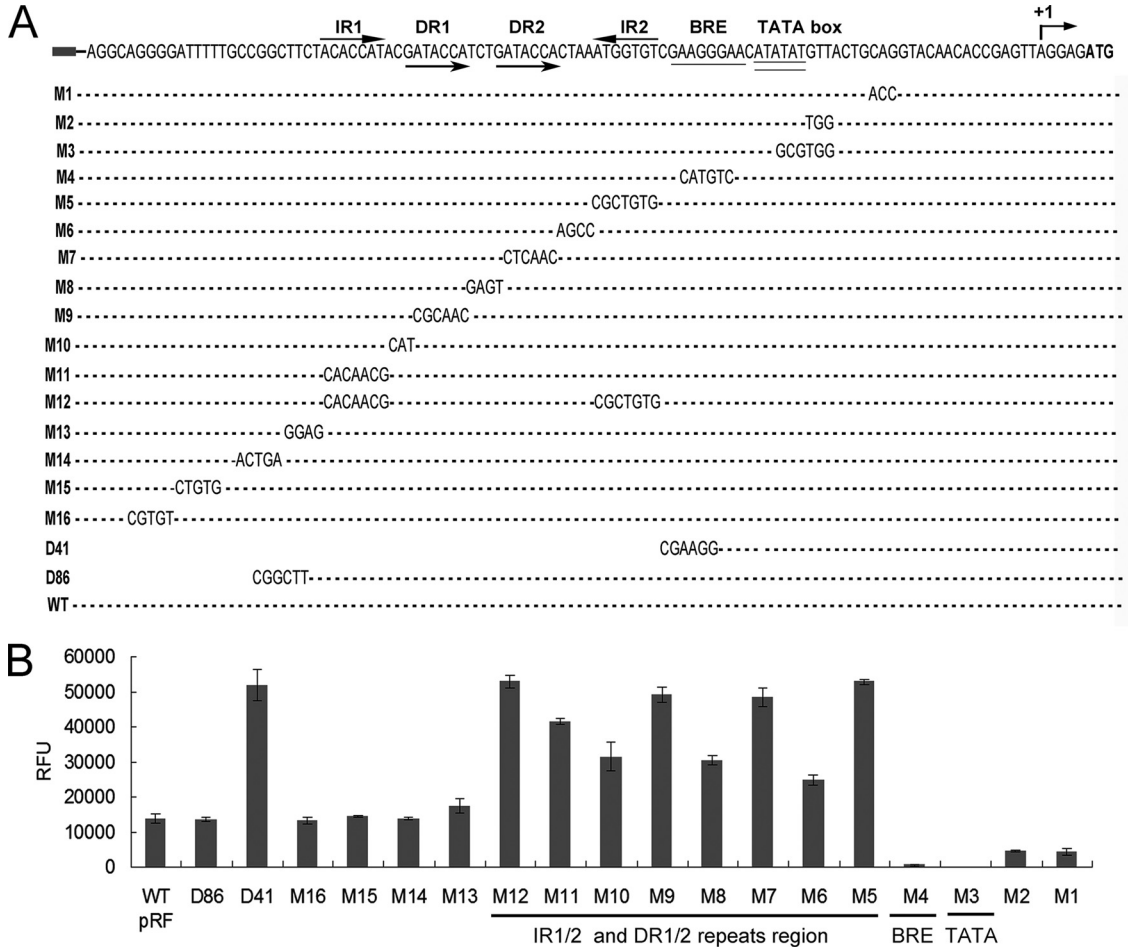

FIG 4 Mapping the core promoter elements and *cis*-elements of the *phaRP* promoter. (A) The sequence of the promoter region of *phaRP* operon is shown on the top. The transcription start site (+1) and the translation start codon are indicated by a bent arrow and boldface letters, respectively. The BRE (single underlined) and TATA box (double underlined) identified by mutagenesis assays are also indicated. The inverted repeat sequences (IR1 and IR2) and the direct repeat sequences (DR1 and DR2) are indicated by arrows. For *phaRP* promoter scanning mutants (M1 to M16), the mutated bases are shown in letters, while the unaltered nucleotides are represented by dashes. The truncation sites in the 5′ deletion mutants (D41 and D86) are shown. The *phaRP* promoter in pRF is defined as the wild-type (WT) promoter. (B) The activities of these mutated promoters of *phaRP* were measured by detecting the fluorescent signal of the reporter GFP. The GFP expression levels of each mutant showed similar increase/decrease profiles (compared with the wild type) between the exponential phase and the stationary phase. For a clear view, only the data collected at the stationary phase are shown. Error bars show standard deviations ($n = 3$).

the *phaRP* promoter *in vivo*. These data indicated that PhaR regulates *phaRP* expression directly through its interaction with the promoter of the *phaRP* operon.

Identification of a specific negative *cis*-element in the promoter of *phaRP* operon. To seek the *cis*-elements important for the inhibition of *phaRP* expression, we introduced mutations into the promoter P_{phaRP} and fused these mutated promoters with the *gfp* reporter gene. After transferring the promoter-*gfp*-fused plasmids (pD41, pD86, and pM1 to pM16) into the DF50 strain, the GFP reporter activities were measured. The P_{phaRP} in the plasmid pRF was taken as the wild-type (WT) promoter (Fig. 1 and 2).

First, the putative core promoter elements, the TATA box and BRE, were found 25 bp upstream of the TSS (Fig. 4). Mutation of the putative TATA box (M3) completely abolished the promoter activity, while mutation of the putative BRE (M4) also caused a significant reduction in the promoter activity (Fig. 4), thus confirming the functional TATA box and BRE of the P_{phaRP} promoter. Interestingly, a truncation mutant, D41, in which only the core promoter portion was left, displayed a remarkably enhanced (approximately 4-fold) promoter activity (Fig. 4). As deletion of the upstream sequence (in D41) significantly weakened or completely abolished the repressive effect to the promoter, this indicated that the negative regulatory elements are located upstream of the core promoter portion.

After analyzing the sequence upstream of the core promoter portion, four repeated sequences were found arrayed in tandem in a region with a length of approximately 40 bp (Fig. 4A). These four repeats were composed of a pair of perfect inverted repeats (IR1 and IR2) as well as a pair of direct repeats (DR1 and DR2). The pair of direct repeats (underlined) (GATACCAN$_3$GATACCA) is flanked by the pair of inverted repeats (underlined) (ACACCATN$_{23}$ ATGGTGT). A truncation mutant, D86, with all four of these repeats reserved exhibited a wild-type promoter activity (Fig. 4). Moreover, the mutation of each repeat induced an increase of 3- to 4-fold in the expression level of P_{phaRP}, whereas the mutation of the spacer sequences between the repeats caused an increase of

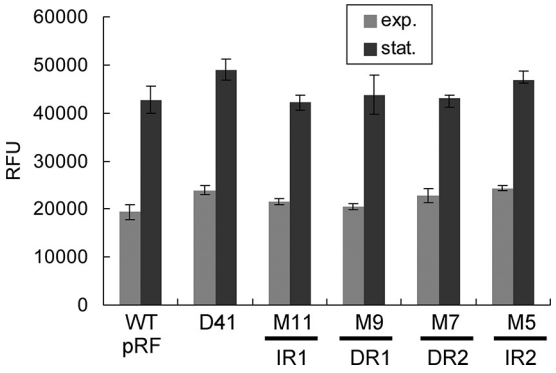

FIG 5 Activities of the representative mutated promoters of the *phaRP* operon in the Δ*phaRPEC* strain. The corresponding mutated regions (IR1/2 and DR1/2) are indicated at the bottom. The *phaRP* promoter in pRF is defined as the wild-type (WT) promoter. The promoter activities in both the exponential (exp.) phase and the stationary (stat.) phase are shown. Error bars show standard deviations ($n = 3$).

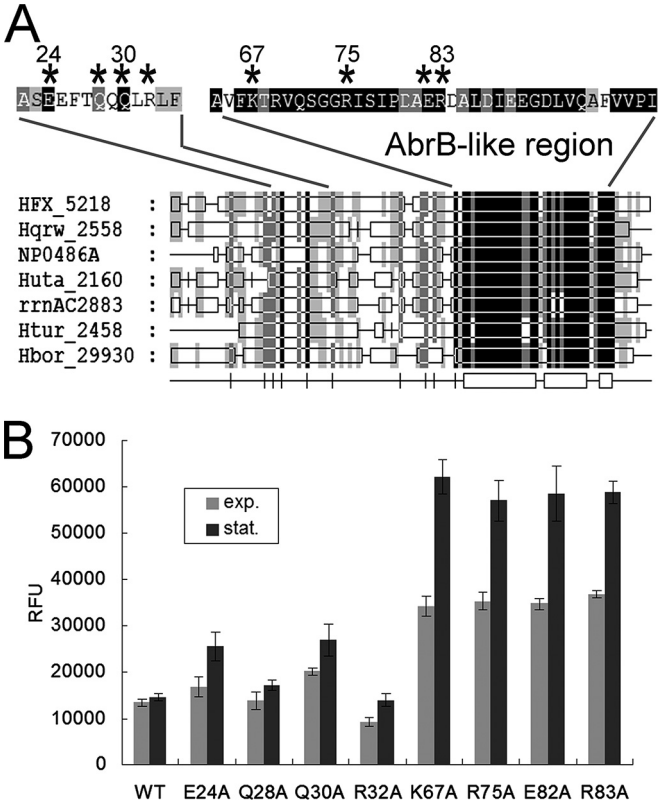

FIG 6 Mutational analysis of several conserved polar amino acid residues of the PhaR protein. (A) Summary view of the multiple alignments of amino acid sequences of PhaR homologs from seven representative haloarchaea species: *H. mediterranei* (HFX), *Haloquadratum walsbyi* (Hqrw), *Natronomonas pharaonis* (NP), *Halorhabdus utahensis* (Huta), *Haloarcula marismortui* (rrnAC), *Haloterrigena turkmenica* (Htur), and *Halogeometricum borinquense* (Hbor). The AbrB-like region is indicated. The residues to be mutated are marked with asterisks. (B) *phaRP* promoter activity assays of mutants with PhaR bearing amino acid substitutions. The residues are indicated in the one-letter amino acid code (E, glutamate; Q, glutamine; R, arginine; K, lysine; and A, alanine). The DF50 strain is indicated as the wild-type (WT) control. The promoter activities in both the exponential (exp.) phase and the stationary (stat.) phase are shown. Error bars show standard deviations ($n = 3$).

approximately 2-fold (Fig. 4). Other mutations introduced into the sequence upstream of this region had almost no effect on the promoter activity (Fig. 4). These results show that each of these four repeated sequences is essential for the repression regulation of *phaRP*, suggesting that the region containing these repeats (IR1/IR2 and DR1/DR2) is the negative *cis*-element and would be the binding position of the transcriptional repressor.

Since PhaR was identified to be a transcriptional repressor of the *phaRP* operon and to interact directly with its promoter *in vivo*, it is most likely that these four repeated sequences of the negative *cis*-element serve as the binding sites of PhaR. To further support this hypothesis, the reporter plasmids with mutations on these four repeats, including pM5, pM7, pM9, pM11, and pD41, were transferred into the Δ*phaRPEC* strains, in which the PhaR was absent, and the promoter activities were measured. As shown in Fig. 5, mutations of those repeats all resulted in high levels of promoter activity similar to that of the wild-type (WT) promoter in pRF. Small increases in the promoter activity were observed in the Δ*phaRPEC* strains containing the plasmid pM5 or pD41, which might be caused by the alteration of the sequence of IR2 that is adjacent to the BRE region. This might promote the recruitment of TFB to BRE and thereby slightly enhanced the transcriptional activity. The mutations of the IR1/IR2 and DR1/DR2 sequences did not cause a significant further enhancement of the expression of *phaRP* in the absence of PhaR, indicating that the four repeated units of the *cis*-element might be the binding sites of PhaR.

The conserved AbrB-like region is critical for the transcriptional repression activity of PhaR. More than 50 homologs of the *H. mediterranei* PhaR were detected by NCBI BLASTp. They were all annotated as conserved hypothetical proteins and were significantly similar, with identities of approximately 50%. The SSDB Gene Cluster Search on KEGG revealed that the *phaR* homologs are located in a similar gene cluster or context at least in 19 species (data from before September 2014), in which only one species, *Natronomonas pharaonis*, lacks the PHA synthase genes and may not accumulate PHA. Interestingly, all 19 species belong to the phylum *Euryarchaeota* of the domain *Archaea*, including one thermophilic archaeon, *Ferroglobus placidus*, and 18 halophilic archaea (see Fig. S2 in the supplemental material). A multiple-alignment analysis of the amino acid sequences of these PhaR homologs revealed that the AbrB-like domain is highly conserved in the C-terminal portion of PhaR homologs (see Fig. S2), indicating an evolutionarily conserved PHA granule-associated regulator unique to archaea.

The high conservation of the AbrB-like domain in PhaR homologs indicated the importance of this domain for PhaR. Several of the highly conserved or charged amino acid residues, E24, Q28, Q30, R32, K67, R75, E82, and R83, in the PhaR protein were mutated, respectively, to alanine to examine the influence of these residues on the repressor function of PhaR (Fig. 6A). These substitution mutations were introduced into the *phaR* gene at its native locus in the genome through homologous recombination. The reporter vector pRF was then introduced into these mutants to assess the repressor activity of these mutated PhaR proteins.

The reporter activities were examined and are shown in Fig. 6B. E24A, Q28A, Q30A, R32A, K67A, R75A, E82A, and R83A refer to the strains with PhaR protein bearing the corresponding amino acid mutations (i.e., E24A is the strain that has the PhaR protein with glutamate replacement with alanine at position 24). The sub-

TABLE 3 PHA accumulation in *H. mediterranei* strains[a]

Strain	PHBV content (% [wt/wt])	3HV fraction (mol%)	Cell dry wt (g/liter)	PHBV concn (g/liter)
DF50	41.79 ± 0.42	8.15 ± 0.21	4.56 ± 0.37	1.9 ± 0.14
Δ*phaRP* mutant	11.89 ± 0.29	5.27 ± 0.06	4.01 ± 0.1	0.48 ± 0.01
Δ*phaRP*/pWL502 mutant	11.05 ± 0.18	3.58 ± 0.15	3.16 ± 0.03	0.35 ± 0
Δ*phaRP*/pWLR mutant	41.93 ± 1.31	6.35 ± 0.17	6.24 ± 0.47	2.62 ± 0.17
Δ*phaRP*/pWLP mutant	33.49 ± 2.36	5.94 ± 0.21	5.91 ± 0.35	1.97 ± 0.06
Δ*phaRP*/pWLRP mutant	42.82 ± 3.2	6.32 ± 0.34	5.97 ± 0.72	2.54 ± 0.13
DF50/pWL502 mutant	49.81 ± 0.52	6.96 ± 0.3	5.02 ± 0.09	2.5 ± 0.07

[a] Cells were cultured at 37°C for 3 days. Data are shown as means ± standard deviations ($n = 3$).

stitutions of alanine for the glutamate, glutamine, and arginine residues in the N-terminal portion of PhaR in the E24A, Q28A, Q30A, and R32A strains only slightly affected the P_{phaRP} activity. In contrast, the K67A, R75A, E82A, and R83A mutants, in which mutations occurred in the C-terminal conserved domain of PhaR, all showed a remarkable increase (2- to 4-fold) in P_{phaRP} activity. These results revealed that PhaR mutants with amino acid substitution in the N-terminal portion still exhibited the capability to suppress the corresponding promoter, whereas, the mutation of the AbrB-like domain of PhaR could significantly weaken or abolish the repressor function of PhaR. These results show that the AbrB-like domain is crucial for the repressor role of PhaR.

It is noteworthy that the expression of the mutated PhaR was driven by the native promoter; thus, the mutant strains might possess different quantities of the mutated PhaR proteins. However, this would not affect our above conclusions on the crucial amino acids of the PhaR. For example, the K67A mutant, which had a high promoter activity of *phaRP* operon, would also produce more $PhaR^{K67A}$. Nevertheless the overproduced $PhaR^{K67A}$ did not result in an enhanced repressive effect on the activity of the P_{phaRP} in the reporter system, further indicating the weakened repressor effect of $PhaR^{K67A}$.

Effect of PhaR on PHA accumulation and PHA granule morphology in *H. mediterranei*. In order to assess the influence of PhaR *in vivo* on the PHA accumulation of *H. mediterranei*, the PHA production capability was investigated in the presence or absence of PhaR. The results showed that when both the phasin PhaP and the phasin regulator PhaR were absent, the *H. mediterranei* strain (Δ*phaRP*) was more deficient in PHA accumulation than the Δ*phaP* strain. The PHA production of the Δ*phaRP* mutant decreased to only approximately 15% to 25% of that of the DF50 strain (Table 3), whereas the Δ*phaP* mutant could maintain a PHA accumulation level of approximately 60% to 70% of that of the DF50 strain (20). The further decrease in the PHA synthesis level was caused by the further knockout of the *phaR* gene, suggesting that PhaR is also very important for PHA synthesis. A similar phenomenon has been reported in *R. eutropha*, in which the PhaR protein was proposed to promote PHA synthesis at least partially through a PhaP-independent pathway (14).

The complementary expression experiments were also performed. The complementary expression of the *phaRP* operon in the Δ*phaRP* strain can restore its PHA accumulation level to that of the wild-type control strain (DF50/pWL502) (Table 3). In addition to the coexpression of *phaRP*, the *phaR* and *phaP* genes were also separately expressed under the control of their native promoter in the plasmids pWLR and pWLP, respectively. The decreased PHA production in the Δ*phaRP* strain was partly restored by the expression of the *phaP* gene, whereas it was surprising that the expression of *phaR* fully restored the high PHA accumulation (Table 3). The results indicated that both PhaP and PhaR could independently promote PHA synthesis.

The effects of PhaR and PhaP on PHA granule morphology were further investigated by TEM (Fig. 7). In the wild-type strains DF50 and DF50/pWL502, most cells harbored multiple moderate-size PHA granules (Fig. 7A and E), whereas in the Δ*phaRP* strain, the cells usually produced only one or two medium-size granules (Fig. 7B). When the *phaR* gene was complementarily expressed in the Δ*phaRP* strain, one or two giant granules were produced in most cells (Fig. 7C), reminiscent of the phenotype of the Δ*phaP* strain (20), indicating that although the PGAP PhaR can recover the high PHA accumulation level and enlarge the PHA granule, PhaR cannot facilitate granule segregation like the major structural protein PhaP. On the other hand, in the Δ*phaRP*/pWLP strain, several small- or medium-size granules with an irregular shape were observed (Fig. 7D). A similar phenotype was exhibited by the Δ*phaRP*/pHP strain, in which *phaP* was overexpressed under the *hsp5* promoter (Fig. 7F). This indicated that the expression of *phaP* without the control of PhaR would cause a disorder in PHA granule formation.

Thus, besides acting as a key transcriptional regulator that controls the amount of PhaP to ensure the formation of regular PHA granules and to facilitate the segregation of granules, the PhaR protein itself is also very important for PHA accumulation and granule formation.

DISCUSSION

To achieve economic production of PHA, increasing studies involved in the metabolic pathways of PHA biosynthesis in haloarchaea have been performed (25, 36), and close attention has also been paid to the global regulation of PHA metabolism, which was explored through proteomic and transcriptomic approaches (37). In this study, we focused on the elucidation of the role of a specific regulator, PhaR, which was identified previously as a small PGAP (12.0 kDa) of *H. mediterranei* (20). Here we demonstrated *in vivo* that PhaR could bind its own promoter specifically and exert an inhibitory effect on the transcription of *phaRP*, suggesting PhaR as the repressor of the phasin gene *phaP* as well as its own gene. In addition, the weaker activity of P_{phaRP} observed in PHA-negative strains implied that the expression level of *phaRP* was also modulated by PHA biosynthesis. Although a similar PHA-sensing regulation strategy was also used by bacteria, *H. mediterranei* has developed a different regulation pattern to achieve such a general smart regulation strategy, with a distinct AbrB-like regulator, PhaR.

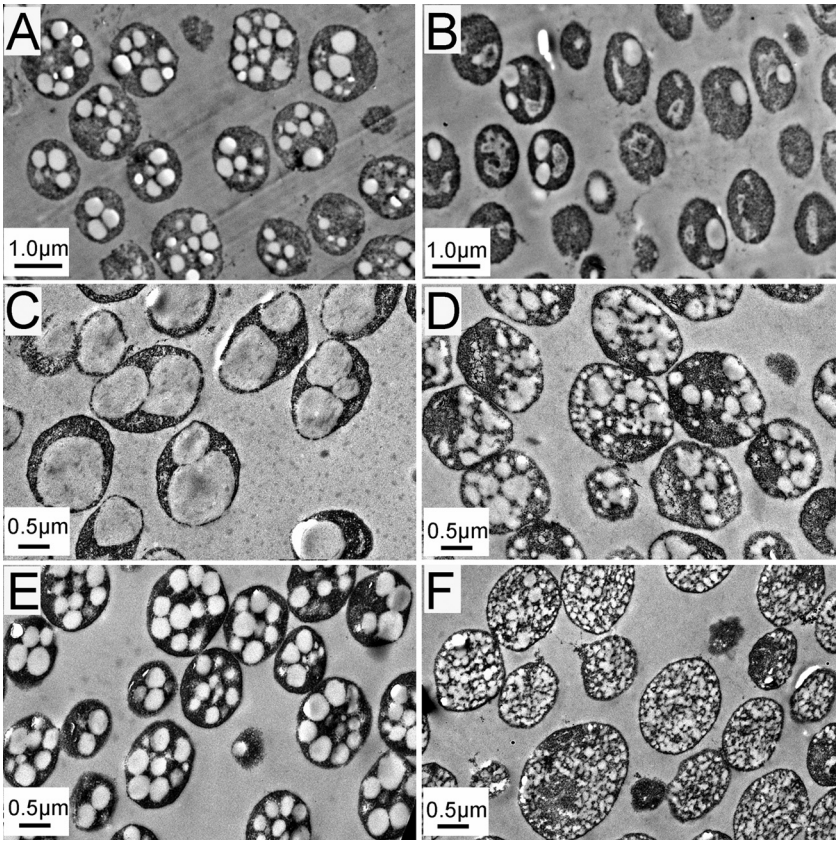

FIG 7 Transmission electron micrographs of PHA granules in *H. mediterranei* strains. (A) *H. mediterranei* DF50 strain; (B) *H. mediterranei* Δ*phaRP* strain; (C) *H. mediterranei* Δ*phaRP*/pWLR strain; (D) *H. mediterranei* Δ*phaRP*/pWLP strain; (E) *H. mediterranei* DF50/pWL502 strain; (F) *H. mediterranei* DF50/pHP strain. The cells were cultivated in MGF medium with uracil added (A and B) or with yeast extract omitted (C to F). The cells were collected during the stationary phase (after cultivation for about 3 days).

First, the regulation pattern of *phaP* by PhaR in *H. mediterranei* is subtly different from that of the bacterial counterpart. In bacteria, the *phaP* gene usually has its own promoter, which is bound by the autoregulator (PhaR) to repress the expression of *phaP* (13, 38, 39). In contrast, in the haloarchaeon *H. mediterranei*, the *phaP* gene overlaps that of the *phaR* gene by 8 bp and the *phaP* is cotranscribed with *phaR* (20). Evidence also showed that there is no independent promoter (20) or independent transcript for *phaP* (Fig. 2C), and PhaR regulates both its own gene and the *phaP* gene simultaneously by binding to their common promoter. These results imply a new regulation pattern for PhaR and PhaP in haloarchaea. A similar regulation pattern was proposed previously in the *phaQ*/*phaP* system in *Bacillus megaterium*. However, a likely *phaP* transcript was observed, and the phasin regulator gene *phaQ* is located far upstream (168 bp) of the *phaP* gene (40). Since 2004, there has been no additional convincing evidence to refute the suggestion presented in 1999 that *B. megaterium phaP* ($phaP_{Bm}$) was also transcribed from a separate promoter (41).

Taking into account the differences in protein level (i.e., that the amount of PhaP is much higher than that of PhaR) and the cotranscriptional expression patterns of the *phaR* and *phaP* genes in *H. mediterranei*, additional regulation might be occurring at the posttranscription levels, such as differences in translational efficiency or protein stability. The codon usage bias analysis provided some insight. For example, all of the three lysine residues of PhaR utilized the lower-frequency codon (AAA), while all of the five lysine residues in PhaP are encoded by the higher-frequency codon (AAG). The codon adaptation index of *phaR* (0.571) is lower than that of *phaP* (0.647). Moreover, the 5′-UTR (AGGAG) of *phaR* is a Shine-Dalgarno (SD)-like sequence, while SD-like sequences (GAGGAAGGAGA) were also found 50 bp upstream of the ATG codon of the *phaP* gene. As reported in chloroplasts, a downstream cistron (*atpE*) of dicistronic mRNAs possesses its own *cis*-element for efficient translation (42); it is likely that *phaP* might also be translated independently, even though there is an overlap (ATGAGTGA) of the *phaR* ORF and the *phaP* ORF. Further research would also be dedicated to the exploration of this multilevel regulation between *phaR* and *phaP* in haloarchaea.

Second, unlike the bacterial phasin regulators PhaR and PhaQ (13, 40, 43), which are predicted to have a helix-turn-helix motif for DNA binding, the *H. mediterranei* PhaR was shown to have a putative DNA-binding motif similar to that of the N-terminal domain of AbrB. AbrB is a small protein (10.2 to 10.6 kDa) that functions as a transition state regulator in *Bacillus* species (44). The N-terminal domains of the AbrB dimmer form a novel fold that was previously called the "looped-hinge helix" (45) and renamed later as the "swapped-hairpin barrel" (34). In addition to various bacteria, this AbrB-like DNA recognition fold is present in archaea, such as the putative chromatin-associated protein Sso7c4 protein in *Sulfolobus solfataricus* (46). The AbrB-like domain of

H. mediterranei PhaR is highly conserved in its archaeal homologs. Several charged residues in this domain, including the positively charged Lys^{67}, Arg^{75}, and Arg^{83} residues, were identified to be crucial, which indicated that these positively charged residues might contribute to DNA binding by interacting with the negatively charged DNA and demonstrated a critical involvement of the AbrB-like domain in the negative regulatory role of the PhaR in *H. mediterranei*. AbrB and AbrB-like proteins usually function as dimers or tetramers (44, 47). In bacteria, PhaR was also shown to form a tetramer *in vitro* (43). In the promoter region of the *phaRP* operon, we identified a specific negative *cis*-element composed of four repeat sequences in tandem (Fig. 4), which are very likely the binding sites of *H. mediterranei* PhaR. In combination with the oligomer character of bacterial PhaR and AbrB, it is implied that the AbrB-like protein PhaR might also function as an oligomer, such as a dimer or a tetramer, to bind the four repeat DNA sequences. Therefore, although they have different DNA-binding motifs, both the haloarchaeal and bacterial PhaRs may regulate the phasin genes by a similar dose-dependent mechanism.

Notably, in addition to the regulation mechanism, the central role of PhaR in PHA accumulation and granule formation in *H. mediterranei* was further addressed in this study. When both of the two major PGAPs PhaR and PhaP were absent, there would be a deficiency in the protection layer between the PHA granule and the cytoplasm, and therefore the cells of the Δ*phaRP* strain could only accumulate a small amount of PHA (Table 3 and Fig. 7B). When only *phaR* was expressed in the Δ*phaRP* strain, PHA accumulation returned to a wild-type level, and the cells synthesized granules larger than those of the Δ*phaRP* strain (Table 3 and Fig. 7C). It is speculated that PhaR might facilitate PHA synthesis in a PhaP-independent mechanism, such as by promoting PHA synthase activity or by acting as the major protein to form a boundary to protect both the PHA and the cytoplasmic protein from unspecific binding. The reason why the Δ*phaRP*/pWLR strain had a higher PHA accumulation level than the Δ*phaP* strain might be the larger amount of PhaR proteins produced by the increased *phaR* gene copy number, as the complementary expression was carried out through a plasmid-based method that increased the gene copy number. When the repressor PhaR was absent, the transcriptional repression effect was released. The sole expression of *phaP* under its native promoter would produce excess PhaP protein. The disordered PHA granule morphology displayed in the Δ*phaRP*/pWLP strain and the DF50/pHP strain (Fig. 7D and F) indicates that the proper amount of PhaP is critical to the formation of regular PHA granules and that it is important to keep the expression of *phaP* under the control of PhaR. Therefore, *H. mediterranei* PhaR, which is essential for the control of the expression of *phaP*, plays a very important role in maintaining proper granule formation.

In summary, our results reveal a novel phasin regulator, PhaR, with a novel regulation pattern in haloarchaea. We demonstrated that in addition to acting as a phasin regulator to control PHA granule morphology, *H. mediterranei* PhaR can also facilitate PHA biosynthesis in a PhaP-independent manner. It is noteworthy that mutation of the promoter of the *phaRP* operon has also generated several very strong promoters that would have potential application in genetic engineering in haloarchaea. Therefore, this study has provided not only new insights into the regulation of PHA synthesis and granule formation in *H. mediterranei* but also the tools and targets for the further exploration and engineering of PHA metabolism in haloarchaea.

ACKNOWLEDGMENTS

We thank Jingnan Liang (Institute of Microbiology, Chinese Academy of Sciences) for technical assistance in the transmission electron microscopy experiments.

This work was supported by grants 31330001 and 31370096 from the National Natural Science Foundation of China.

REFERENCES

1. **Lee SY.** 1996. Bacterial polyhydroxyalkanoates. Biotechnol Bioeng **49:**1–14. http://dx.doi.org/10.1002/(SICI)1097-0290(19960105)49:1<1::AID-BIT1>3.3.CO;2-1.
2. **Steinbüchel A, Füchtenbusch B.** 1998. Bacterial and other biological systems for polyester production. Trends Biotechnol **16:**419–427. http://dx.doi.org/10.1016/S0167-7799(98)01194-9.
3. **Fernandez-Castillo R, Rodriguez-Valera F, Gonzalez-Ramos J, Ruiz-Berraquero F.** 1986. Accumulation of poly(beta-hydroxybutyrate) by halobacteria. Appl Environ Microbiol **51:**214–216.
4. **Han J, Hou J, Liu H, Cai S, Feng B, Zhou J, Xiang H.** 2010. Wide distribution among halophilic archaea of a novel polyhydroxyalkanoate synthase subtype with homology to bacterial type III synthases. Appl Environ Microbiol **76:**7811–7819. http://dx.doi.org/10.1128/AEM.01117-10.
5. **Legat A, Gruber C, Zangger K, Wanner G, Stan-Lotter H.** 2010. Identification of polyhydroxyalkanoates in *Halococcus* and other haloarchaeal species. Appl Microbiol Biotechnol **87:**1119–1127. http://dx.doi.org/10.1007/s00253-010-2611-6.
6. **Anderson AJ, Dawes EA.** 1990. Occurrence, metabolism, metabolic role, and industrial uses of bacterial polyhydroxyalkanoates. Microbiol Rev **54:**450–472.
7. **Griebel R, Smith Z, Merrick JM.** 1968. Metabolism of poly-beta-hydroxybutyrate. I. Purification, composition, and properties of native poly-beta-hydroxybutyrate granules from *Bacillus megaterium*. Biochemistry **7:**3676–3681.
8. **Jendrossek D, Pfeiffer D.** 2014. New insights in formation of polyhydroxyalkanoate (PHA) granules (carbonosomes) and novel functions of poly(3-hydroxybutyrate) (PHB). Environ Microbiol **16:**2357–2373. http://dx.doi.org/10.1111/1462-2920.12356.
9. **Pötter M, Steinbüchel A.** 2005. Poly(3-hydroxybutyrate) granule-associated proteins: impacts on poly(3-hydroxybutyrate) synthesis and degradation. Biomacromolecules **6:**552–560. http://dx.doi.org/10.1021/bm049401n.
10. **Pfeiffer D, Wahl A, Jendrossek D.** 2011. Identification of a multifunctional protein, PhaM, that determines number, surface to volume ratio, subcellular localization and distribution to daughter cells of poly(3-hydroxybutyrate), PHB, granules in *Ralstonia eutropha* H16. Mol Microbiol **82:**936–951. http://dx.doi.org/10.1111/j.1365-2958.2011.07869.x.
11. **Galán B, Dinjaski N, Maestro B, de Eugenio LI, Escapa IF, Sanz JM, García JL, Prieto MA.** 2011. Nucleoid-associated PhaF phasin drives intracellular location and segregation of polyhydroxyalkanoate granules in *Pseudomonas putida* KT2442. Mol Microbiol **79:**402–418. http://dx.doi.org/10.1111/j.1365-2958.2010.07450.x.
12. **Rehm BH.** 2006. Genetics and biochemistry of polyhydroxyalkanoate granule self-assembly: the key role of polyester synthases. Biotechnol Lett **28:**207–213. http://dx.doi.org/10.1007/s10529-005-5521-4.
13. **Pötter M, Madkour MH, Mayer F, Steinbüchel A.** 2002. Regulation of phasin expression and polyhydroxyalkanoate (PHA) granule formation in *Ralstonia eutropha* H16. Microbiology **148:**2413–2426.
14. **York GM, Stubbe J, Sinskey AJ.** 2002. The *Ralstonia eutropha* PhaR protein couples synthesis of the PhaP phasin to the presence of polyhydroxybutyrate in cells and promotes polyhydroxybutyrate production. J Bacteriol **184:**59–66. http://dx.doi.org/10.1128/JB.184.1.59-66.2002.
15. **Tian JM, He AM, Lawrence AG, Liu PH, Watson N, Sinskey AJ, Stubbe J.** 2005. Analysis of transient polyhydroxybutyrate production in *Wautersia eutropha* H16 by quantitative Western analysis and transmission electron microscopy. J Bacteriol **187:**3825–3832. http://dx.doi.org/10.1128/JB.187.11.3825-3832.2005.
16. **Yamada M, Yamashita K, Wakuda A, Ichimura K, Maehara A, Maeda M, Taguchi S.** 2007. Autoregulator protein PhaR for biosynthesis of poly-

hydroxybutyrate [P(3HB)] possibly has two separate domains that bind to the target DNA and P(3HB): functional mapping of amino acid residues responsible for DNA binding. J Bacteriol **189:**1118–1127. http://dx.doi.org/10.1128/JB.01550-06.

17. **Pötter M, Müller H, Steinbüchel A.** 2005. Influence of homologous phasins (PhaP) on PHA accumulation and regulation of their expression by the transcriptional repressor PhaR in *Ralstonia eutropha* H16. Microbiology **151:**825–833. http://dx.doi.org/10.1099/mic.0.27613-0.
18. **Zhao D, Cai L, Wu J, Li M, Liu H, Han J, Zhou J, Xiang H.** 2013. Improving polyhydroxyalkanoate production by knocking out the genes involved in exopolysaccharide biosynthesis in *Haloferax mediterranei*. Appl Microbiol Biotechnol **97:**3027–3036. http://dx.doi.org/10.1007/s00253-012-4415-3.
19. **Koller M, Hesse P, Bona R, Kutschera C, Atlić A, Braunegg G.** 2007. Potential of various archae- and eubacterial strains as industrial polyhydroxyalkanoate producers from whey. Macromol Biosci **7:**218–226. http://dx.doi.org/10.1002/mabi.200600211.
20. **Cai S, Cai L, Liu H, Liu X, Han J, Zhou J, Xiang H.** 2012. Identification of the haloarchaeal phasin (PhaP) that functions in polyhydroxyalkanoate accumulation and granule formation in *Haloferax mediterranei*. Appl Environ Microbiol **78:**1946–1952. http://dx.doi.org/10.1128/AEM.07114-11.
21. **Sambrook J, Russell DW.** 2001. Molecular cloning: a laboratory manual, 3rd ed. Cold Spring Harbor Laboratory Press, Cold Spring Harbor, NY.
22. **Liu H, Han J, Liu X, Zhou J, Xiang H.** 2011. Development of *pyrF*-based gene knockout systems for genome-wide manipulation of the archaea *Haloferax mediterranei* and *Haloarcula hispanica*. J Genet Genomics **38:**261–269. http://dx.doi.org/10.1016/j.jgg.2011.05.003.
23. **Krebs MP, Mollaaghababa R, Khorana HG.** 1993. Gene replacement in *Halobacterium halobium* and expression of bacteriorhodopsin mutants. Proc Natl Acad Sci U S A **90:**1987–1991. http://dx.doi.org/10.1073/pnas.90.5.1987.
24. **Reuter CJ, Maupin-Furlow JA.** 2004. Analysis of proteasome-dependent proteolysis in *Haloferax volcanii* cells, using short-lived green fluorescent proteins. Appl Environ Microbiol **70:**7530–7538. http://dx.doi.org/10.1128/AEM.70.12.7530-7538.2004.
25. **Hou J, Feng B, Han J, Liu HL, Zhao DH, Zhou J, Xiang H.** 2013. Haloarchaeal-type beta-ketothiolases involved in poly(3-hydroxybutyrate-*co*-3-hydroxyvalerate) synthesis in *Haloferax mediterranei*. Appl Environ Microbiol **79:**5104–5111. http://dx.doi.org/10.1128/AEM.01370-13.
26. **Miao D, Sun C, Xiang H.** 2009. Construction and application of a novel shuttle expression vector based on haloarchaeal plasmid pSCM201. Wei Sheng Wu Xue Bao **49:**1040–1047. (In Chinese.)
27. **Cline SW, Lam WL, Charlebois RL, Schalkwyk LC, Doolittle WF.** 1989. Transformation methods for halophilic archaebacteria. Can J Microbiol **35:**148–152. http://dx.doi.org/10.1139/m89-022.
28. **Cai L, Cai SF, Zhao DH, Wu JH, Wang L, Liu XQ, Li M, Hou J, Zhou J, Liu JF, Han J, Xiang H.** 2014. Analysis of the transcriptional regulator GlpR, promoter elements, and posttranscriptional processing involved in fructose-induced activation of the phosphoenolpyruvate-dependent sugar phosphotransferase system in *Haloferax mediterranei*. Appl Environ Microbiol **80:**1430–1440. http://dx.doi.org/10.1128/AEM.03372-13.
29. **Lu Q, Han J, Zhou L, Coker JA, DasSarma P, DasSarma S, Xiang H.** 2008. Dissection of the regulatory mechanism of a heat-shock responsive promoter in haloarchaea: a new paradigm for general transcription factor directed archaeal gene regulation. Nucleic Acids Res **36:**3031–3042. http://dx.doi.org/10.1093/nar/gkn152.
30. **Kuhn J, Binder S.** 2002. RT-PCR analysis of 5′ to 3′-end-ligated mRNAs identifies the extremities of *cox2* transcripts in pea mitochondria. Nucleic Acids Res **30:**439–446. http://dx.doi.org/10.1093/nar/30.2.439.
31. **Han J, Lu Q, Zhou L, Zhou J, Xiang H.** 2007. Molecular characterization of the $phaEC_{Hm}$ genes, required for biosynthesis of poly(3-hydroxybutyrate) in the extremely halophilic archaeon *Haloarcula marismortui*. Appl Environ Microbiol **73:**6058–6065. http://dx.doi.org/10.1128/AEM.00953-07.
32. **Wilbanks EG, Larsen DJ, Neches RY, Yao AI, Wu CY, Kjolby RAS, Facciotti MT.** 2012. A workflow for genome-wide mapping of archaeal transcription factors with ChIP-seq. Nucleic Acids Res **40:**e74. http://dx.doi.org/10.1093/nar/gks063.
33. **Tian J, Sinskey AJ, Stubbe J.** 2005. Kinetic studies of polyhydroxybutyrate granule formation in *Wautersia eutropha* H16 by transmission electron microscopy. J Bacteriol **187:**3814–3824. http://dx.doi.org/10.1128/JB.187.11.3814-3824.2005.
34. **Coles M, Djuranovic S, Söding J, Frickey T, Koretke K, Truffault V, Martin J, Lupas AN.** 2005. AbrB-like transcription factors assume a swapped hairpin fold that is evolutionarily related to double-psi beta barrels. Structure **13:**919–928. http://dx.doi.org/10.1016/j.str.2005.03.017.
35. **Lu QH, Han J, Zhou LG, Zhou J, Xiang H.** 2008. Genetic and biochemical characterization of the poly(3-hydroxybutyrate-*co*-3-hydroxyvalerate) synthase in *Haloferax mediterranei*. J Bacteriol **190:**4173–4180. http://dx.doi.org/10.1128/JB.00134-08.
36. **Han J, Hou J, Zhang F, Ai GM, Li M, Cai SF, Liu HL, Wang L, Wang ZJ, Zhang SL, Cai L, Zhao DH, Zhou J, Xiang H.** 2013. Multiple propionyl coenzyme A-supplying pathways for production of the bioplastic poly(3-hydroxybutyrate-*co*-3-hydroxyvalerate) in *Haloferax mediterranei*. Appl Environ Microbiol **79:**2922–2931. http://dx.doi.org/10.1128/AEM.03915-12.
37. **Liu H, Luo Y, Han J, Wu J, Wu Z, Feng D, Cai S, Li M, Liu J, Zhou J, Xiang H.** 2013. Proteome reference map of *Haloarcula hispanica* and comparative proteomic and transcriptomic analysis of polyhydroxyalkanoate biosynthesis under genetic and environmental perturbations. J Proteome Res **12:**1300–1315. http://dx.doi.org/10.1021/pr300969m.
38. **Maehara A, Taguchi S, Nishiyama T, Yamane T, Doi Y.** 2002. A repressor protein, PhaR, regulates polyhydroxyalkanoate (PHA) synthesis via its direct interaction with PHA. J Bacteriol **184:**3992–4002. http://dx.doi.org/10.1128/JB.184.14.3992-4002.2002.
39. **Chou ME, Yang MK.** 2010. Analyses of binding sequences of the PhaR protein of *Rhodobacter sphaeroides* FJ1. FEMS Microbiol Lett **302:**138–143. http://dx.doi.org/10.1111/j.1574-6968.2009.01836.x.
40. **Lee TR, Lin JS, Wang SS, Shaw GC.** 2004. PhaQ, a new class of poly-beta-hydroxybutyrate (PHB)-responsive repressor, regulates *phaQ* and *phaP* (phasin) expression in *Bacillus megaterium* through interaction with PHB. J Bacteriol **186:**3015–3021. http://dx.doi.org/10.1128/JB.186.10.3015-3021.2004.
41. **McCool GJ, Cannon MC.** 1999. Polyhydroxyalkanoate inclusion body-associated proteins and coding region in *Bacillus megaterium*. J Bacteriol **181:**585–592.
42. **Suzuki H, Kuroda H, Yukawa Y, Sugiura M.** 2011. The downstream *atpE* cistron is efficiently translated via its own *cis*-element in partially overlapping *atpB-atpE* dicistronic mRNAs in chloroplasts. Nucleic Acids Res **39:**9405–9412. http://dx.doi.org/10.1093/nar/gkr644.
43. **Maehara A, Doi Y, Nishiyama T, Takagi Y, Ueda S, Nakano H, Yamane T.** 2001. PhaR, a protein of unknown function conserved among short-chain-length polyhydroxyalkanoic acids producing bacteria, is a DNA-binding protein and represses *Paracoccus denitrificans phaP* expression in vitro. FEMS Microbiol Lett **200:**9-15. http://dx.doi.org/10.1111/j.1574-6968.2001.tb10685.x.
44. **Chumsakul O, Takahashi H, Oshima T, Hishimoto T, Kanaya S, Ogasawara N, Ishikawa S.** 2011. Genome-wide binding profiles of the *Bacillus subtilis* transition state regulator AbrB and its homolog Abh reveals their interactive role in transcriptional regulation. Nucleic Acids Res **39:**414–428. http://dx.doi.org/10.1093/nar/gkq780.
45. **Vaughn JL, Feher V, Naylor S, Strauch MA, Cavanagh J.** 2000. Novel DNA binding domain and genetic regulation model of *Bacillus subtilis* transition state regulator abrB. Nat Struct Biol **7:**1139–1146. http://dx.doi.org/10.1038/81999.
46. **Hsu CH, Wang AH.** 2011. The DNA-recognition fold of Sso7c4 suggests a new member of SpoVT-AbrB superfamily from archaea. Nucleic Acids Res **39:**6764–6774. http://dx.doi.org/10.1093/nar/gkr283.
47. **Yao F, Strauch MA.** 2005. Independent and interchangeable multimerization domains of the AbrB, Abh, and SpoVT global regulatory proteins. J Bacteriol **187:**6354–6362. http://dx.doi.org/10.1128/JB.187.18.6354-6362.2005.